

# Shock waves in ultracold Fermi (Tonks) gases

Bogdan Damski

*Instytut Fizyki, Uniwersytet Jagielloński, ul. Reymonta 4, PL-30-059 Kraków, Poland*

It is shown that a broad density perturbation in a Fermi (Tonks) cloud takes a shock wave form in the course of time evolution. A very accurate analytical description of shock formation is provided. A simple experimental setup for the observation of shocks is discussed.

Shock waves show up in various physical systems. For example, we find them in a gas bubble driven acoustically, in a photonic crystal, and even in a Bose-Einstein condensate [1]. In this Letter we study properties of shock waves in ultracold Fermi (Tonks) gases: the simplest many-body quantum system. To this aim, we consider dynamics of a Gaussian-like density perturbation being initially at rest on the fermionic cloud. We show that such a perturbation divides into two pieces that travel in opposite directions in the course of free time evolution. The two perturbations change their shape during propagation, and eventually two shock wave fronts are formed [2]. We provide a detailed theoretical description of their formation and further propagation.

Experimental studies of such phenomena are possible due to recent progress in cooling and trapping of fermionic gases [3]. What's more, it turns out that interparticle interactions between cold trapped fermions are negligible [3], making the theoretical description exactly tractable.

Another exactly solvable many-body system is related to one-dimensional (1D) hard-core bosonic gas, the so called Tonks gas [4, 5, 6]. As suggested by Olshanii *et al.* [5] tightly confined alkali atoms are very promising candidates for experimental realization of the Tonks gas.

There is a close connection between Tonks and 1D Fermi gases due to the Fermi-Bose mapping theorem (FBMT) [4, 6]. This theorem says that if  $\Psi(x_1, \dots, x_N)$  is the ground state of the  $N$ -fermion system described by (dimensionless) Hamiltonian

$$\hat{H} = \sum_{i=1}^N \left[ -\frac{1}{2} \frac{\partial^2}{\partial x_i^2} + V(x_i) \right], \quad (1)$$

then the exact many-body ground state Tonks wave function, in an external potential the same as in (1), is  $\prod_{1 \leq j < k \leq N} \text{sign}(x_k - x_j) \Psi(x_1, \dots, x_N)$  [4, 6]. As a result, the single-particle density

$$\varrho_N(x) = \int dx_2 \cdots dx_N |\Psi(x, x_2, \dots, x_N)|^2 \quad (2)$$

is identical for Fermi and Tonks clouds. Since FBMT can be extended to time dependent problems [6], density perturbations on Fermi and Tonks clouds propagate *exactly* the same way.

It was proposed by Kolomeisky and Straley that quantitative features of Tonks (Fermi) density profile can be

correctly addressed by the mean-field approach [7], where density  $\varrho_N(x) \approx |\Phi(x)|^2$  with  $\Phi(x)$  being the ground state solution of

$$-\frac{1}{2} \frac{\partial^2}{\partial x^2} \Phi(x) + V(x)\Phi(x) + \frac{G}{2} |\Phi(x)|^4 \Phi(x) = \mu \Phi(x), \quad (3)$$

with  $G = \pi^2 N^2$ ,  $N \gg 1$ , and  $|\Phi(x)|^2$  normalized to unity. On the basis of (3) we find a distance over which the density profile tends to its bulk value  $\rho$  when subjected to a localized perturbation. This characteristic length scale is called the healing length  $\xi(\rho)$ , and equals  $1/\sqrt{G\rho}$ . A natural extension of (3) allows for time dependent studies according to

$$i \frac{\partial}{\partial t} \Phi(x, t) = \left( -\frac{1}{2} \frac{\partial^2}{\partial x^2} + V + \frac{G}{2} |\Phi|^4 \right) \Phi(x, t). \quad (4)$$

Therefore, a many-body character of the problem has been overcome by introducing nonlinearity into the theoretical description.

In this Letter, we investigate formation of shocks and their dynamics using both the mean-field approach (4) and the exact many-body treatment [8]. We show that the mean-field formalism allows for accurate *analytical* determination of all the quantities concerning shock formation. Explicit comparison of the mean-field results to the exact calculations allows us to specify the range of applicability of Eq. (4). After shock creation the mean-field approach becomes inaccurate, and our discussion is based solely on exact findings.

To begin, the dynamics of an initial density perturbation in a 1D system will be described. This perturbation can be produced by an adiabatic focusing of an appropriately detuned laser beam on the particles [9]. Alternatively, one may cool the cloud in the presence of a laser beam [10]. We assume that our system consists of a zero temperature Fermi (Tonks) gas. Atoms are placed in a 1D periodic box having boundaries at  $x = \pm l$ .

In the Thomas-Fermi regime, when the kinetic energy term in (3) is negligible, density profile takes form

$$|\Phi(x, 0)|^2 = \rho_0 \sqrt{1 + 2\alpha e^{-x^2/2\sigma^2}}, \quad (5)$$

where we assume that the laser produces potential  $u_0 \exp(-x^2/2\sigma^2)$ , with  $\xi(\rho_0) \ll \sigma \ll l$ , and  $\alpha \propto u_0$ . We determine  $\rho_0$  from the condition  $\int dx |\Phi(x, 0)|^2 = 1$ . For  $\alpha \leq 0.5$  density profile can be rewritten as follows

$$|\Phi(x, 0)|^2 \approx \rho_0 + \rho_0 (\sqrt{1 + 2\alpha} - 1) e^{-x^2/2\kappa^2}, \quad (6)$$

where  $\kappa = \sigma \int dx (\sqrt{1 + 2\alpha e^{-x^2}} - 1) / (\sqrt{1 + 2\alpha} - 1) \sqrt{\pi}$  provides a correct normalization of (6).

Suppose that the laser beam has been abruptly turned off and the perturbation (6) starts to evolve. If the system was described by a single-particle Schrödinger equation, the perturbation would spread out. To find out what happens in a many-body problem first we consider the low amplitude limit. The “wave function” is written as  $\Phi(x, t) = e^{-i\mu t} [\Phi_0 + \delta\Phi(x, t)]$ , where  $\Phi_0 = 1/\sqrt{2l}$  and  $\mu = N^2\pi^2/8l^2$ . The density profile reads

$$|\Phi(x, t)|^2 = \Phi_0^2 + \Phi_0[\delta\Phi(x, t) + \delta\Phi^*(x, t)] + O(|\delta\Phi|^2). \quad (7)$$

For  $\alpha \rightarrow 0$  we find, with the help of (5) and (7), that

$$\delta\Phi(x, 0) = \alpha\Phi_0(e^{-x^2/2\sigma^2} - \sigma\sqrt{2\pi}/2l)/2 + O(\alpha^2). \quad (8)$$

The linearization of (4) leads to the equation

$$i\frac{\partial}{\partial t}\delta\Phi = -\frac{1}{2}\frac{\partial^2}{\partial x^2}\delta\Phi + G\Phi_0^4(\delta\Phi + \delta\Phi^*),$$

which can be solved by means of Bogoliubov substitution:  $\delta\Phi(x, t) = \sum_n a_n [u_n(x)e^{-i\omega_n t} + v_n^*(x)e^{i\omega_n t}]$ . Straightforward calculation determines modes  $u_n$ ,  $v_n$  and frequencies  $\omega_n$ . Coefficients  $\{a_n\}$  are found from the initial condition (8). Substitution of  $\delta\Phi(x, t)$  into (7) gives

$$|\Phi(x, t)|^2 = \Phi_0^2 + \alpha\sigma\Phi_0^2\sqrt{2\pi} \sum_{n=1} e^{-k_n^2\sigma^2/2} \cos(k_n x) \cos(\omega_n t)/l + O(\alpha^2), \quad (9)$$

where  $\omega_n = k_n \sqrt{c_0^2 + k_n^2/2}$ ,  $c_0 = \sqrt{G}\Phi_0^2$ , and  $k_n = n\pi/l$ . Approximating  $\omega_n \approx k_n c_0$  ( $\sigma \gg 1/c_0$ ), and changing summation into integration we arrive at

$$|\Phi(x, t)|^2 \approx \Phi_0^2 - \alpha\Phi_0^2\sqrt{2\pi}\sigma/2l + \alpha\Phi_0^2[e^{-(x-c_0t)^2/2\sigma^2} + e^{-(x+c_0t)^2/2\sigma^2}]/2 + O(\alpha^2). \quad (10)$$

Thus, we see that the initial density profile breaks into two separate pieces moving with the sound velocity  $c_0$  in the opposite directions. The dynamics of these perturbations will be the subject of subsequent considerations. Finally, notice that the whole discussion applies to systems with  $N \gg 1$  (see (3)).

Having in mind the low amplitude result, a hydrodynamical approach, that fully accounts for nonlinear character of the problem, will be developed. We write “wave function”  $\Phi$  as  $\sqrt{\rho} \exp(i\chi)$  and define the velocity field:  $v = \partial_x \chi$ . Eq. (4) in  $(\rho, v)$  variables for a homogeneous system takes form

$$\frac{\partial \rho}{\partial t} + \frac{\partial}{\partial x}(v\rho) = 0, \quad (11)$$

$$\frac{\partial v}{\partial t} + \frac{\partial}{\partial x}\left(\frac{1}{2}v^2\right) + \frac{\partial}{\partial x}\left(\frac{G}{2}\rho^2 - \frac{1}{2}\frac{\partial_x^2 \sqrt{\rho}}{\sqrt{\rho}}\right) = 0, \quad (12)$$

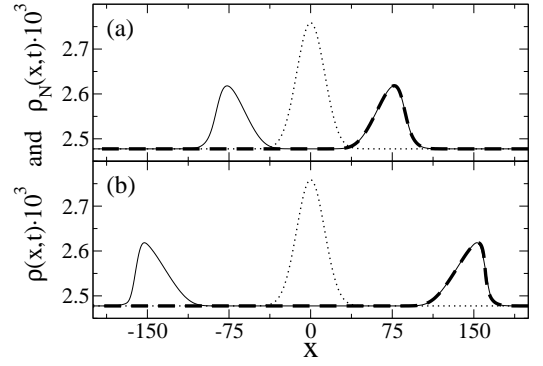


FIG. 1: Density of atoms as a function of time. Dotted line corresponds to  $\rho_N(x, 0)$ . Solid line is the exact  $N$ -fermion solution [8], and a dashed line is the analytical approximation (13). Plot (a) [(b)] is for  $t = 22.2$  [44.4]. Parameters:  $\alpha = 0.12$ ,  $u_0 \approx -1.16$ ,  $\sigma = 12.5$ ,  $\kappa \approx 12.7$ ,  $N = 399$ ,  $l = 200$ , see [11] for units.

where (11) is a continuity equation, while (12) is similar to the Euler equation from classical hydrodynamics. To simplify the problem we will neglect in (12) the so called quantum pressure (QP) term  $\sim \partial_x^2 \sqrt{\rho}/\sqrt{\rho}$  [9]. Simple estimation shows that it is of the order of  $1/s^2$  with  $s$  being the typical spatial scale of variations of the density profile. Therefore, it is important when  $\rho^2 G \sim 1/s^2$ , which means that  $s$  is of the order of the healing length  $\xi$ . We assume that initially a perturbation is broad:  $s \gg \xi$ .

Solution of a similar problem in classical hydrodynamics is known for years [2]. Following [2] we find exact traveling wave solutions of (11) and (12) (without the QP term)

$$\rho = f(x - (a_0 \pm 2\sqrt{G}\rho)t) \quad , \quad v = a_0 \pm \sqrt{G}\rho,$$

where  $f$  (an arbitrary function) and  $a_0$  (a constant) can be found from initial conditions. The sign  $\pm$  determines a direction of propagation. This solution is qualitatively the same as the one obtained for the ideal 1D gas [2], where the existence of shocks is well known.

We aim at the determination of dynamics of a single Gaussian-like profile moving to the right. Analytical solution of a full problem seems to be very difficult due to the lack of superposition principle. On the basis of the low amplitude result (10), we assume that initially the right moving part is a Gaussian of half-amplitude of the initial perturbation (6), and impose a natural condition that  $v(x \rightarrow \pm l, 0) \rightarrow 0$ . It yields to

$$\rho(x, t) = \rho_0 + \rho_0 \eta \exp(-[x - \sqrt{G}(-\rho_0 + 2\rho)t]^2/2\kappa^2), \quad (13)$$

with  $\eta = (\sqrt{1 + 2\alpha} - 1)/2$  (6). We would like to stress that (13) holds for an arbitrary large  $\eta$  since we fully account for the nonlinear term. Many interesting results can be obtained from (13) despite its implicit form.

First, the maximum of the impulse has a constant amplitude equal to  $\rho_0(1 + \eta)$  and moves with a constant velocity  $\mathcal{V}(\eta) = \sqrt{G\rho_0}(1 + 2\eta)$ . For  $\eta \rightarrow 0$  we get  $\mathcal{V}_0 \approx \sqrt{G\rho_0} = c_0$ , which is the speed of sound propagating at the background density  $\rho_0$ . In this limit we recover (10).

Second, bright perturbations ( $\eta > 0$ ) move with higher velocity,  $\mathcal{V}(\eta)$ , than dark structures ( $\eta < 0$ ). This simple prediction could be directly verified experimentally. Moreover, it is in a qualitative agreement with numerical simulations of Karpiuk *et al.* [12, 13], even though they generate excitations in a quite different way.

Third, the shape of the perturbation changes in the course of time evolution – Fig. 1. Since the speed of propagation increases with density, the upper part of bright impulse moves faster than its tail leading to self-steepening in the direction of propagation. Eventually, shock will be formed, i.e.  $\partial\rho(x)/\partial x = -\infty$  in at least one point of the profile.

To determine time and position of shock formation we solve the set of equations [2]

$$\frac{\partial x(\rho)}{\partial \rho} = 0 \quad , \quad \frac{\partial^2 x(\rho)}{\partial \rho^2} = 0. \quad (14)$$

The first one is equivalent to  $|\partial\rho(x)/\partial x| = \infty$ , and the second one is necessary to assure uniqueness of  $\rho(x)$ . For the density profile (13) one easily finds  $x(\rho)$  and solves (14). Without the loss of generality we assume from now on that  $\eta > 0$ , and find time  $t_s$  of shock formation, and density  $\rho_s$  at which shock appears

$$t_s = \frac{\kappa}{2\sqrt{G\rho_0}\eta e^{-1/2}} \quad , \quad \rho_s = \rho_0 + \rho_0\eta e^{-1/2}. \quad (15)$$

As a result, an initially broad Gaussian-like density perturbation moving in the Fermi (Tonks) cloud (13) develops a shock wave front during time evolution. This is the central result of our paper. The solution (10) fails to predict such behavior, since it is derived in the zero amplitude limit ( $\eta \rightarrow 0$ ) where  $t_s \rightarrow \infty$ .

Interestingly, the time of shock formation can be correctly estimated without solving (14). Indeed, the half-width of the impulse ( $\approx 2\kappa$ ) is a difference in a distance traveled by the upper and lower parts of the impulse until shock appears:  $2\kappa \approx (\mathcal{V}(\eta) - \mathcal{V}_0)t_s$ . It gives  $t_s \sim \kappa/\sqrt{G\eta\rho_0}$ . Estimating the position of a shock wave front by position of impulse's maximum we get a very simple expression:  $x_s = \kappa e^{1/2}(1 + 1/2\eta)$ .

Comparison of the analytical solution (13) to the  $N$ -body one [8] for a moderately large initial perturbation ( $x_s > l$ ) shows excellent agreement—see Fig. 1. As  $x_s$  becomes smaller than half-box-size ( $= l$ ) shock waves show up in our simulations. We have increased the amplitude of the initial perturbation and compared a full mean-field calculation with the exact fermionic one [8]. As shown in Fig. 2, until the expected moment of shock wave creation agreement is very good. The analytical solution

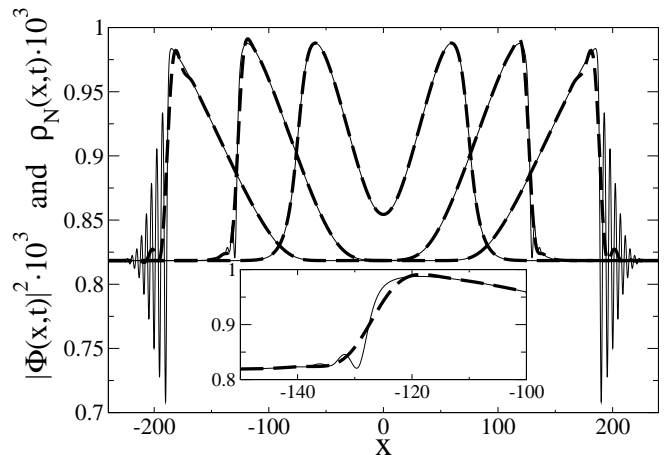


FIG. 2: Density of atoms as a function of time. Subsequent profiles correspond to  $t = 41, 82, 131.2$ . Dashed line is an exact  $N$ -body calculation [8], while solid line presents numerical solution of mean-field equation (4). Inset shows details of a density profile at  $t = 82$ . Shock's characteristics:  $t_s = 81.6$  and  $x_s = 118.4$ . Parameters:  $\alpha = 0.5$ ,  $u_0 \approx -0.53$ ,  $\sigma = 20$ ,  $l = 600$ ,  $N = 399$ ,  $\xi(0.8 \cdot 10^{-3}) \approx 1$ , see [11] for units.

(13), not presented in Fig. 2, fits nicely to exact calculation as long as  $t < t_s$ . Then, the mean field approach fails to reproduce exact calculations at the *front* edge, and non-physical atom oscillations appear. We found that the QP term, playing a role when a spatial scale of density variations ( $s$ ) becomes comparable to the healing length  $\xi$ , is responsible for their appearance. As  $t$  tends to  $t_s$  we find  $s \rightarrow \xi$  (Fig. 2). Therefore, we find that the dynamical mean-field approach (4) works nicely as long as  $s \gg \xi$  and fails when  $s \sim \xi$ . In this way we bring a quantitative criteria into discussion [6, 14] concerning applicability of the Kolomeisky and Straley equation (4) to Tonks (Fermi) systems.

Although, the derivative of density does not exactly go to infinity, the density profile becomes very steep at the front edge – Fig. 2. To look more quantitatively at shocks' dynamics we define the symmetry coefficient  $\Lambda$  as  $\int_{x_m}^l dx[\rho_N(x) - \rho_N(l)] / \int_0^{x_m} dx[\rho_N(x) - \rho_N(l)]$ , i.e. as a ratio between the number of atoms in the front and rear impulse's parts with respect to the impulse maximum being at  $x_m > 0$ .  $\Lambda$  is close to zero for a well developed shock wave profile, and equals to one for symmetric perturbations.

In the first stage of evolution, the profile undergoes self-steepening dynamics so that  $\Lambda$  decreases reaching the lowest value approximately at  $t = t_s = 81.6$  – Fig. 2, 3b. Then  $\Lambda(t)$  decreases a little and becomes flat – impulse propagates roughly without change of shape until  $t \approx 150$  (Fig. 2, 3b). In the course of further evolution a shock wave front gradually disappears and the density profile becomes more and more symmetric ( $\Lambda \rightarrow 1$ ) – Fig. 3a. Therefore, we conclude that there are three stages of

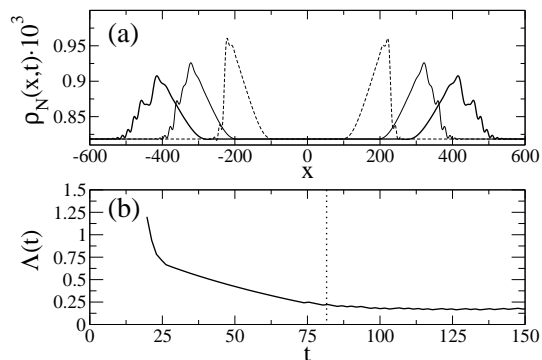


FIG. 3: Plot (a): further time evolution of the density profile from Fig. 2. Subsequent profiles correspond to  $t = 164, 262.4, 344.4$ . Plot (b): symmetry coefficient  $\Lambda(t)$ . Dotted line shows expected moment of the shock formation. Both plots present exact  $N$ -body results [8]. Parameters: as in Fig. 2, see [11] for units.

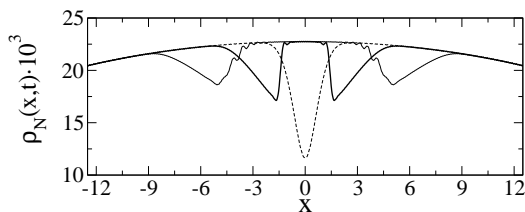


FIG. 4: The exact many-body time evolution of the density profile of  $N = 399$  fermions in a harmonic trap [8]. Subsequent profiles correspond to  $t = 0, 4\pi/120, 9\pi/120$  ( $2\pi$  is a trap period) [15]. Notice that for dark perturbations back edge self-steepens instead of the front one. Parameters:  $\sigma = 0.75, u_0 = 300$ .

evolution: the shock wave formation, propagation of a shock-like impulse, and the impulse *explosion* leading to broadening of the density profile.

Finally, let us comment on the dynamics of density perturbations in a harmonically trapped case:  $V(x_i) = x_i^2/2$  (1). The division of an initial density perturbation into two similar pieces happens independently of the location of the laser beam focus. Just after the laser turn off the two perturbations travel in opposite directions to the edge of the cloud and come back to join after half-trap-period. At this moment the density profile is a mirror image of the initial shape. Then another splitting takes place and the dynamics repeats itself. As in the homogeneous case, perturbations undergo self-steepening dynamics leading to formation of a shock-like front, which then blows up – Fig. 4.

Quasi-one-dimensional atomic traps form very promising systems for observation of shock waves. Indeed, their reduced dimensionality avoids dispersion of the impulse amplitude due to multidimensional propagation. The periodicity of shocks formation in a harmonic trap should allow for their multiple *in situ* observations [10] in a single run of an experiment.

It is worthwhile to point out that the described splitting of the initial perturbation has been already experimentally observed in a Bose-Einstein condensate (BEC) [10]. An extension of our calculations to Bose gases provides a theoretical description of a shock formation in a BEC. These results are presented in [16].

To summarize, we have studied in detail dynamics of density wave packets in the Fermi (Tonks) cloud. We have derived a simple analytical expression for the speed of propagation of Gaussian-like density wave packets having *arbitrary* amplitude. This result can be crucial for determination of the sound velocity from experimental data. We have also described analytically the process of a shock wave formation, and proposed a simple experimental setup for its observation. This prediction can be *directly* verified in a single run of experiment. Finally, we have found that the “quantum” shock wave front blows up at some point instead of becoming more and more steep in the course of free time evolution. The presence of shock waves in three-dimensional configurations can be an interesting subject for future studies. Indeed, as pointed out in [13], the propagation of density perturbations in a three-dimensional Fermi gas can differ significantly from a quasi-one-dimensional case. The hydrodynamical approach proposed in [13] supported by exact many-body calculations can be used for such investigations.

I would like to acknowledge discussions with M. Brewczyk, Z. P. Karkuszewski, K. Sacha, and J. Zakrzewski. Work supported by KBN project 2 P03B 124 22.

- 
- [1] M. P. Brenner, S. Hilgenfeld, and D. Lohse, Rev. Mod. Phys. **74**, 425 (2002); E. J. Reed, M. Soljačić, and J. D. Joannopoulos, Phys. Rev. Lett. **90**, 203904 (2003); Z. Dutton, M. Budde, C. Slowe, and L. V. Hau, Science **293**, 663 (2001).
  - [2] L. D. Landau and E. M. Lifshitz, Fluid Mechanics (Pergamon 1995).
  - [3] B. DeMarco and D. S. Jin, Science **285**, 1703 (1999); A. G. Truscott *et al.*, Science **291**, 2570 (2001); F. Schreck *et al.*, Phys. Rev. Lett. **87**, 080403 (2001).
  - [4] M. D. Girardeau and E. M. Wright, Laser Phys. **12**, 8 (2002).
  - [5] M. Olshanii, Phys. Rev. Lett. **81**, 938 (1998); V. Dunjko, V. Lorent, and M. Olshanii, *ibid.* **86**, 5413 (2001).
  - [6] M. D. Girardeau and E. M. Wright, Phys. Rev. Lett. **84**, 5239 (2000).
  - [7] E. B. Kolomeisky and J. P. Straley, Phys. Rev. B **46**, 11749 (1992); E. B. Kolomeisky, T. J. Newman, J. P. Straley, and X. Qi, Phys. Rev. Lett. **85**, 1146 (2000).
  - [8] We find the  $N$  lowest eigenstates of the Hamiltonian  $-\frac{1}{2} \frac{\partial^2}{\partial x^2} + V(x) + u_0 \exp(-x^2/2\sigma^2)$  [ $V(x) = 0$  or  $x^2/2$ ]. After laser turn off ( $u_0 = 0$ ) they undergo an ordinary single-particle time evolution. The many-body Fermi wave function is a Slater determinant built out of them.

- [9] C. J. Pethick and H. Smith, *Bose-Einstein Condensation in Dilute Gases*, (Cambridge University Press 2002).
- [10] M. R. Andrews, D. M. Kurn, H. J. Meisner, D. S. Durfee, C. G. Townsend, S. Inouye, and W. Ketterle, *Phys. Rev. Lett.* **79**, 553 (1997).
- [11] Since we consider here a homogeneous system, we take arbitrary length scale  $l_0$  for a unit of length. For a unit of time we choose  $ml_0^2/\hbar$ , where  $m$  is the atomic mass.
- [12] T. Karpiuk, M. Brewczyk, L. Dobrek, M. A. Baranov, M. Lewenstein, and K. Rzażewski, *Phys. Rev. A* **66**, 023612 (2002).
- [13] T. Karpiuk, M. Brewczyk, and K. Rzażewski, *J. Phys. B* **35**, L315 (2002).
- [14] E. B. Kolomeisky, T. J. Newman, J. P. Straley, and X. Qi, *Phys. Rev. Lett.* **86**, 4709 (2001).
- [15] We use here the harmonic oscillator units where a unit of length equals  $\sqrt{\hbar/m\omega}$  and a unit of time is  $1/\omega$ . Naturally,  $\omega$  is a trap frequency and  $m$  is an atomic mass. For example, taking a realistic case of  $\omega = 2\pi \cdot 10\text{Hz}$ , density profiles in Fig. 4 correspond to  $t = 0, 1.7\text{ms}, 3.8\text{ms}$ .
- [16] B. Damski, e-print cond-mat/0309421.